Synthesis of reduced graphene oxide decotate Cu_2S nanoparticles for cathode of quantum dot solar cell

Le Doan Duy[1], Le Thi Ngoc Tu[2], Le Tien Dat[3]
[1]Faculty of Basic Sciences, Vinh Long University of Technology Education, Vinh Long City, Vinh Long Province, Viet Nam
[2]Faculty of Natural Sciences, Dong Thap University, Cao Lanh City, Viet Nam
[3]Faculty of Basic Sciences, University of Cuu Long, Vinh Long City, Vinh Long Province, Viet Nam

Article Info

ABSTRACT

In this paper, the results of making a reduced graphene oxide cathode electrode with Cu_2S nanoparticles are shown so that it can be used as a counter electrode in quantum dot solar cells to replace other counter electrodes. An rGO-Cu_2S paste obtained by hydrolysis was scanned onto the surface of the fluorine-doped tin oxide (FTO) conductive substrate when bound to Cu_2S nano by a screen-printing process, then calcined at 350 °C to crystallize the film. Following calcination, the film was examined for structure using energy-dispersive X-ray (EDX) and X-ray diffraction (XRD) spectroscopy, as well as for type and particle size using scanning and transmission electron microscopy and transmission electron microscopy, respectively. Mott-schottky measurement is used to determine the semiconductor and carrier concentrations in the film, and an electrochemical device is used to assess the electrodes redox capacity in a polysulfide electrolyte solution. The operability of the rGO-Cu_2S cathode at the peak of the current density in the C-V curve was 24 mA/cm^2, a 30-fold increase compared to that of the Cu_2S electrode. This result shows that the efficiency, Voc, FF, Jsc are 4.92%, 0.525 V, 0.418, and 22.4 mA/cm^2, respectively.

Corresponding Author:

Le Thi Ngoc Tu
Faculty of Natural Sciences, Dong Thap University
783, Pham Huu Lau Road, Sward 6, Dong Thap City, Viet Nam
Email: ltntu@dthu.edu.vn

1. INTRODUCTION

Quantum dot solar cells, often referred to as quantum dot-sensitized solar cells, or QDSSCs, have been developed using a variety of QDs, including CdS, CdSe, PbS, PbSe, and InP [1], [2]. The quantum dots offer a number of advantages over dye molecules, such as the capacity to absorb multiple exciton pairs, the ability to change the bandgap energy by modifying the particle size [3], and a higher optical absorption coefficient than dye molecule particles [4], QDSSCs now have a photoelectric conversion efficiency (DSSCs) that is inferior to dye-sensitized solar cells [5]–[9].

They only partially absorb sunlight and do not fully exploit the visible spectrum because the incredible efforts [9]–[11] were caried out on single CdS or CdSe nanomaterials. In specifically, the bulk materials absorption wavelengths for CdS and CdSe are respectively 550 and 705 nm. Both materials absorption wavelengths are much shorter at the QD size than the values indicated above. After using the binding agent, the performance did not notice a significant improvement. In order to havest the efficiency, a UV-Vis spectrum of photoanodes must expand in the visible light region. Therefore, a combining CdS/CdSe nanoscrystal had been caried out using numerous organizations using single QDs [12]–[15].

The counter electrode (CE), which receives electrons from the external circuit and restores the electrolyte through a redox process at the surface of the electrolyte and CE, was the subject of research in addition to that on the photoanode electrode because CE is crucial to improving the performance of QDSSCs. Therefore, a cathode must have a high porosity level in order for CE to have a large surface area of contact with the electrolyte system, a large conductivity, and a high level of electrochemical activity, which will aid in the electrolyte systems redox processes occurring more quickly, being chemically stable, and being less expensive [16].

The counter electrode (CE), which receives electrons from the external circuit and restores the electrolyte through a redox process. Therefore, a cathode must have a high porosity level in order for CE to have a large surface area of contact with the electrolyte system, a large conductivity, and a high level of electrochemical activity, which will aid in the electrolyte systems redox processes occurring more quickly, being chemically stable, and being less expen researchers have searched for CEs that may achieve the aforementioned features over the years in an effort to replace the conventional CE Pt. Metal sulfide compounds such Mo2S [17], PbS [18], NiS [19], FeS [20], CuS [21], and Cu2S [12] have been shown to be capable of meeting the aforementioned criteria and replacing CE Pt. Copper sulfide (CuS, Cu2S) is employed for more investigations than the other materials in this category because it possesses a Eg of 1.1–1.4 eV, high electrochemical activity, and stability in polysulfide [22]–[24]. In order to create CEs, Cu thin films with a thickness of a few micrometers are submerged in a polysulfide. However, as immersing in a long time, the copper brass will continue to breakdown (the CuS or Cu2S film will thicken), generating a large resistance, lowering FF and Voc, and decreasing efficiency. QDSSC yield is also decreased [22]–[24].

To develop suitable negative electrodes, several kinds of carbon have been explored recently [25]–[28]. Due to its substantial surface area, excellent conductivity, affordable manufacture, and environmental friendliness, a reduced graphene oxide is a contender to take the position of conventional negative electrodes [29]. An electrochimical properties is also significantly influenced by crystal defects or -COOH or -OH functional groups [30], [31]. Since there is no link between the layers of graphenes multilayer structure, each layer is typically incredibly thin-roughly the size of an atom. As a result, we frequently need to dope graphene with other beneficial electrochemical materials like CuS, Cu2S, and MoS2 to generate a graphene cathode with a suitably large porous [25], [32]–[35]. According to the studies mentioned above, the combination of rGO and Cu2S materials generally has many benefits over other materials, making it particularly suited to be employed as a cathode for QDSSCs. In this study, we make use of rGOs advantageous transmission characteristics to assist and speed up the movement of electrons from the external circuit through counter electrodes into the electrolyte system while minimizing losses.

2.   EXPERIMENTAL DETAILS

Materials: sigma of germany provided the supplies, which included graphene oxide (GO), ethylene glycol, CuCl, thioure, polyvinylpyrrolidone (PVP), ethanol, polyethylene glycol (PEG), and substrate fluorine-doped tin oxide (FTO).

−   Fabricated processes

A mixture of 20 ml of ethylene glycol mixed with 0.1 M CuCl and 0.1 M thioure (CH4N2S structure), 12 mg of GO powder dissolved in 8 ml of ethanol, and 0.5 grams of PVP were produced. A complicated combination was agitated for 30 minutes at room temperature to produce a gray solution. To create a green solution, the mixture was left in an autoclave for 24 hours at 180 °C. Once at room temperature, rinse with ethanol and distilled water. The product was heated in the oven for 12 hours at 60 °C. Finally, a paste was created by swirling the aforementioned product with 10 ml of ethanol and 1.2 g of PEG at room temperature. To create the FTO/rGO-Cu2S cathode, the paste was then screen printed onto the FTO conductive substrate and heated for 40 minutes at 350 °C.

−   Characterization

To determine the surface shape and particle size, we used high-resolution scanning electron microscopy (FE-SEM) and transmission electron microscopy (TEM). FTIR spectroscopy and X-ray diffraction (XRD) are used to obtain the structure of the film. The components, elements, and percentages of the elements in the film are also determined using energy dispersive spectroscopy, which when combined with FTIR and XRD will provide us with a picture of the structure of the manufactured material. We can measure the Mott-Schottky to ascertain the semiconductor type and carrier concentration in CEs and measure the cyclic electrochemical potential curve of the cathode electrode in the solution thanks to the electrochemical impedance spectroscopy (EIS) equipment. To evaluate how well the negative electrode is working, use the polysulfide solution S2-/Sn2-.

3. RESULTS AND DISCUSSION

The results of the energy-dispersive X-ray (EDX) spectroscopy method, as shown in Figure 1, are used to determine the composition of the sample. The characteristic energy peaks for the elements C and O-2.1 keV for carbon and 1.6 keV for oxygen-appear on the corresponding EDX spectrum. The conductive glass substrates Si element as well as the measurement electrodes Au and Cu elements are among the additional elements that are present.

The percentages of elements present in the sample are listed in Table 1. The results show that the GO sample consists of two main elements: carbon and oxygen. Where the mass percent of carbon is 69.6% and that of the element oxygen is 2.4%.
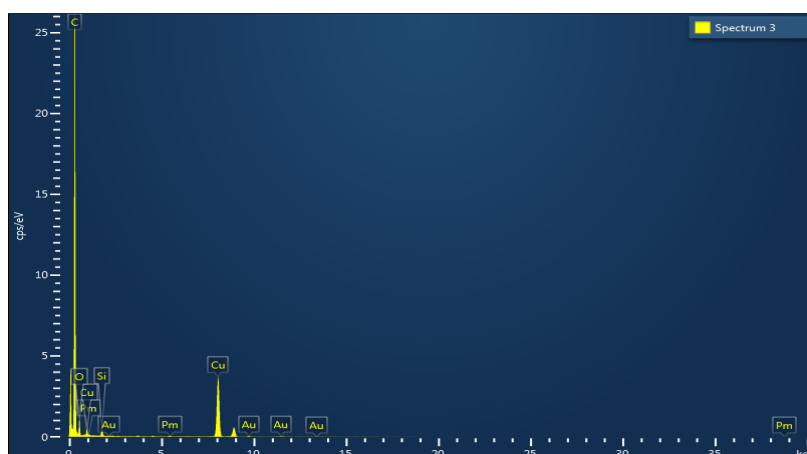

Figure 1. EDX of GO powder

Table 1. The composition of elements in the GO sample

Elements	Radiant energy level	Energy peak (KeV)	Mass ratio (%)
C	K	2.1	69.6
O	K	1.6	2.4

X-ray diffraction was used to determine a structural rGO/Cu_2S film that made by the hydrothermal method at 180 °C for 24 hours. Figure 2 shows the XRD of rGO/Cu_2S powder. There were diffraction peaks of Cu_2S at diffraction angle positions of 27.2°, 35.7°, and 48.1°, corresponding to planes with miller indices (100), (102), and (110), respectively, in accordance with the standard [36], and diffraction peaks of CuS at diffraction angle positions of 33.4° and 52.7°, which correspond to planes with Miller indices (103), (108), which are consistent with JCPDS standard number 79-2321 and rGOs diffraction peaks at 22.8° and 41.4°, respectively, and correspond to planes with Miller indices of (002), (001) [34].
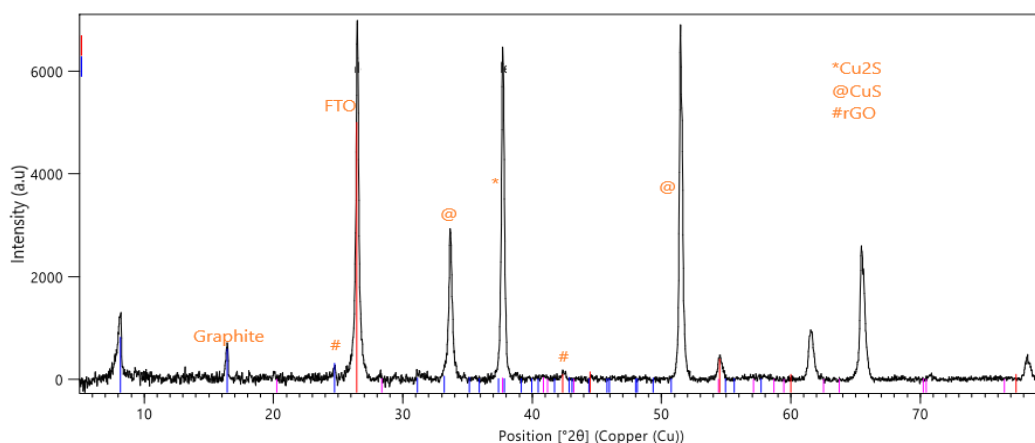

Figure 2. XRD of an $FTO/rGO-Cu_2S$ counter electrode

Morphologies of the rGO and rGO-Cu2S films on the FTO substrate, characterized by FE-SEM Figures 3(a) and (b). The rGO film showed that rGO has a spherical shape, the size is unevenly distributed, and 100 to 400 nm-size, containing many voids and porosity Figure 3(a). After rGO binds with Cu2S nanoparticles, the porosity of the film decreases, and rGO and Cu2S particles bind together to form a composite block.
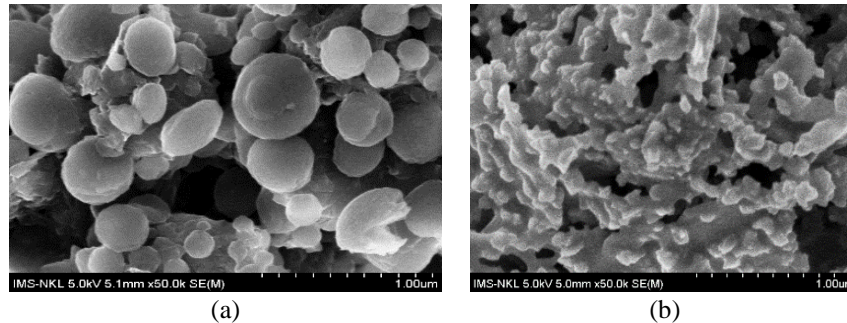

| (a) | (b) |

Figure 3. FE-SEM of (a) FTO/rGO and (b) FTO/rGO-Cu2S counter electrode

An electrochemical device is used to assess the carrier concentration and semiconductor type of manufactured materials using the Mott-Schottky method [37], [38]. EC-Lab software was used to fit and identify the semiconductor type and carrier concentration matching to the region of the manufactured film after measuring Mott-Schottky (0.196 cm2). In (1) tells us how to figure out the concentration of N carriers in the film:

$$\frac{1}{C_{sc}^2} = \frac{2}{e\varepsilon\varepsilon_o N}\left(E - E_{FB} - \frac{kT}{e}\right)$$

(1)

Where C_{sc} is the capacitance of the film, D is the dielectric constant, and εo is the electrical constant, E is the measured potential value of the electrode, and E_{FB} is determined when the tangent line to the graph intersects the horizontal axis where $C = 0$, k is Boltzmanns constant, e is the elemental charge, and T is the ambient temperature.

From the fit results obtained in Figure 4, the ambient temperature is 25 °C, the area of the fabrication electrode is 0.196 cm2, the E_{FB} is -1.752 V, the frequency is 10.015 kHz, and the carrier concentration of $0.466.10^{24}$ cm-3 is obtained corresponds to an n-type semiconductor. The large values of N facilitate the electrochemical processes at the surface of the cathode electrode with the polysulfide electrolyte system.
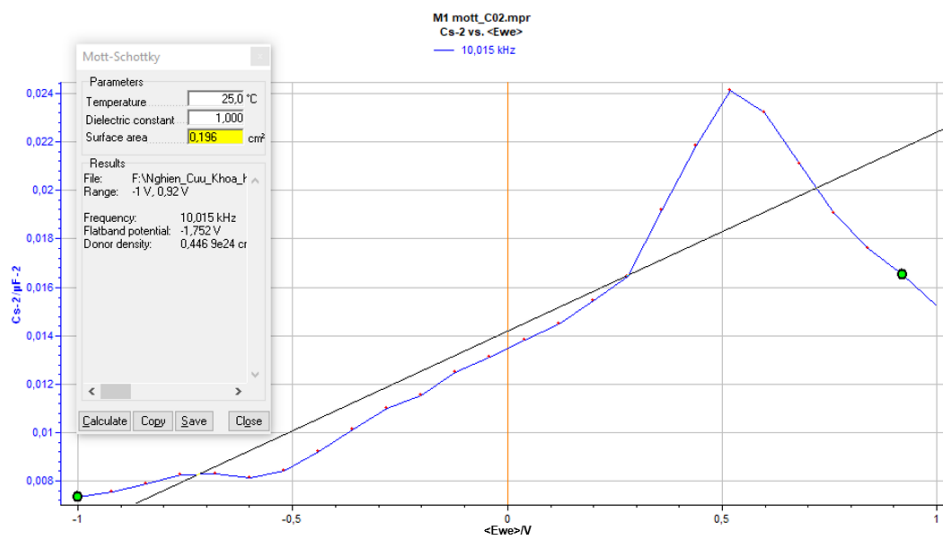

Figure 4. Fitted mott-schottky graph

According to the results of the structural study discussed above, Cu2S material formed on the FTO film and was connected to the rGO materials lattice. We used an electrochemical cyclic potential scan to get the electrodes current and corresponding potential in order to analyze the electrochemical activity of the cathode electrode and the oxidation-reduction process using S2-/Sn2- electrolyte [39]. The Figure 5 shows C-V curves of Pt, rGO-Cu2S and rGO counter electrodes. Both electrodes operate in the solution of the polysulfide electrolyte system shown in Figures 3(a) and (b). In the C-V spectrum, the positive peak is the oxidation of S2- ions to Sn2-, and the negative peak corresponds to the reduction of Sn2- ions to S2- [40], [41]. The size of the C-V peak serves as a measure of the electrodes quality; the larger the peak, the better the electrodes ability to transfer excited charges to S2-/Sn2- electrolyte and lessen electron loss processes at the electrical surface extreme [42], [43]. The oxidation peak of the rGO-Cu2S electrode was found to be approximately 6 mA, which is approximately 30 times that of the Pt electrode and 12 times that of rGO electrodes. The oxidation peak of the Pt electrode was approximately 0.2 mA. This finding demonstrates that the rGO-Cu2S electrode has superior electrochemical characteristics to the Pt electrode. In the previous study by tung group and colleagues, they successfully fabricated a Cu2S cathode electrode with a photoelectric conversion efficiency of 3.77%, many times higher than other cathode electrodes such as Pt or PbS [44].
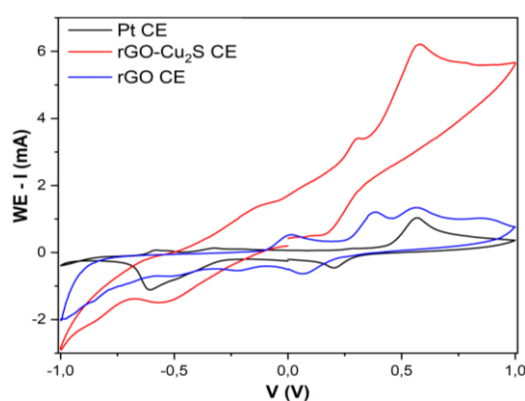

Figure 5. C-V curve of Pt, rGO-Cu2S and rGO counter electrodes

In this study, the QDSSCs were created using an electrode that contained a significant amount of GO. Surlyn, the polysulfide electrolyte system employed for cell operation, bonds the photoanode and cathode electrodes of QDSSCs together. We test the batteries conversion efficiency using a voltage and current density curve as shown in Figure 6. A 100 mW/cm2 solar spectrum simulation light is flashed, it indicators Jsc, Voc, FF, and efficiency of 4.92%, Voc of 0.525 V, FF of 0.418, and Jsc of 22.4 mA/cm2, among other data. It has a better efficiency than both the Pt counter electrode (2.05%, 0.47 V, 0.328, and 13.3 mA/cm2) and the rGO (3.98%, 0.515 V, 0.4, and 19.3 mA/cm2).
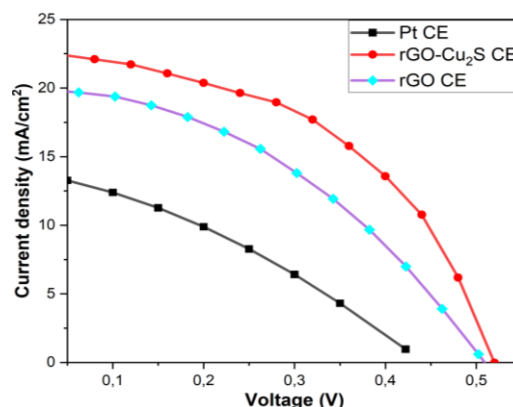

Figure 6. J-V curve measurement of QDSSCs with Pt and FTO/rGO-Cu2S CEs

Figure 7 is the electrochemical resistance spectrum of QDSSCs with the FTO/rGO-Cu2S CEs. The purpose of measuring EIS is to obtain a dynamic resistance when it operates under the influence of light. From Figure 7, we can see the resistance values Rct1 (resistance across the surface of CEs/electrolyte and diffusion of electrons in the electrolyte) and Rct2 (resistance across the surface of TiO2/QDs and diffusion resistance inside the electrolyte and the TiO2 semiconductor film). Here, by studying the influence of the FTO/rGO-Cu2S counter electrode component, we focus on Rct1. As a result, after fitting the experimental impedance spectrum, we determined the value of Rct1 to be 10.9 Ω. It is smaller than that of Pt (46.7 Ω) and rGO (21.8 Ω) counter electrode. This value also is very small if compared with the results of Phuong *et al*. [44].
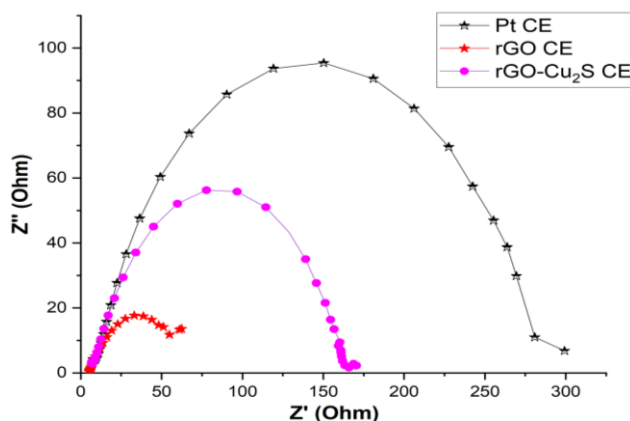

Figure 7. EIS of QDSSCs with an FTO/rGO-Cu2S counter electrode

4. CONCLUSION

The rGO-Cu2S cathodes have successfully synthesized using the hydrothermal method and screen-printing technique on a FTO conductive substrate; the active area is 0.196 cm2. The morphology of the film was determined by TEM and FE-SEM with a very porous rGO surface; the diameter of the layers is about 2-3 μm, the average-sized Cu2S nanoparticles of around 20 nm are linked on the rGO lattice. The structure of the electrode was determined by X-ray diffraction, EDX, and FTIR spectroscopy. Besides, we use the electrochemical system to determine the n-type rGO-Cu2S electrode from mott-schottky, with carrier concentration of 0.466.1024 cm-3. The operability of the rGO-Cu2S cathode at the peak of the current density in the C-V curve was 6 mA, a 30-fold increase compared to that of the Pt electrode. This result shows the outstanding capability of the electrode corresponding to efficiency, Voc, FF and Jsc of 4.92 %, 0.525 V, 0.418, and 22.4 mA/cm2.

REFERENCES

[1]   A. Zaban, O. I. Mićić, B. A. Gregg, and A. J. Nozik, "Photosensitization of nanoporous TiO2 electrodes with InP quantum dots," *Langmuir*, vol. 14, no. 12, pp. 3153–3156, Jun. 1998, doi: 10.1021/la9713863.
[2]   P. Yu, K. Zhu, A. G. Norman, S. Ferrere, A. J. Frank, and A. J. Nozik, "Nanocrystalline TiO2 solar cells sensitized with InAs quantum dots," *Journal of Physical Chemistry B*, vol. 110, no. 50, pp. 25451–25454, Dec. 2006, doi: 10.1021/jp064817b.
[3]   W. W. Yu, Y. A. Wang, and X. Peng, "Formation and Stability of Size-, Shape-, and Structure-Controlled CdTe Nanocrystals: Ligand Effects on Monomers and Nanocrystals," *Chemistry of Materials*, vol. 15, no. 22, pp. 4300–4308, Nov. 2003, doi: 10.1021/cm034729t.
[4]   M. C. Beard, "Multiple exciton generation in semiconductor quantum dots," *Journal of Physical Chemistry Letters*, vol. 2, no. 11, pp. 1282–1288, Jun. 2011, doi: 10.1021/jz200166y.
[5]   J. Fang, J. Wu, X. Lu, Y. Shen, and Z. Lu, "Sensitization of nanocrystalline TiO2 electrode with quantum sized CdSe and ZnTCPc molecules," *Chemical Physics Letters*, vol. 270, no. 1–2, pp. 145–151, May 1997, doi: 10.1016/S0009-2614(97)00333-3.
[6]   W. Lee *et al.*, "Spectral broadening in quantum dots-sensitized photoelectrochemical solar cells based on CdSe and Mg-doped CdSe nanocrystals," *Electrochemistry Communications*, vol. 10, no. 11, pp. 1699–1702, Nov. 2008, doi: 10.1016/j.elecom.2008.08.025.
[7]   D. Liu and P. V. Kamat, "Photoelectrochemical behavior of thin CdSe and coupled TiO2/CdSe semiconductor films," *Journal of Physical Chemistry*, vol. 97, no. 41, pp. 10769–10773, Oct. 1993, doi: 10.1021/j100143a041.
[8]   A. N. Jumabekov *et al.*, "Comparison of Solid-State Quantum-Dot-Sensitized Solar Cells with ex Situ and in Situ Grown PbS Quantum Dots," *Journal of Physical Chemistry C*, vol. 118, no. 45, pp. 25853–25862, Nov. 2014, doi: 10.1021/jp5051904.
[9]   R. Vogel, K. Pohl, and H. Weller, "Sensitization of highly porous, polycrystalline TiO2 electrodes by quantum sized CdS," *Chemical Physics Letters*, vol. 174, no. 3–4, pp. 241–246, Nov. 1990, doi: 10.1016/0009-2614(90)85339-E.
[10]   I. Mora-Seró *et al.*, "Factors determining the photovoltaic performance of a CdSe quantum dot sensitized solar cell: The role of the linker molecule and of the counter electrode," *Nanotechnology*, vol. 19, no. 42, p. 424007, Oct. 2008, doi: 10.1088/0957-4484/19/42/424007.
[11]   Y. J. Shen and Y. L. Lee, "Assembly of CdS quantum dots onto mesoscopic TiO2 films for quantum dot-sensitized solar cell

applications," *Nanotechnology*, vol. 19, no. 4, p. 045602, Jan. 2008, doi: 10.1088/0957-4484/19/04/045602.

[12] Y. L. Lee and Y. S. Lo, "Highly efficient quantum-dot-sensitized solar cell based on co-sensitization of CdS/CdSe," *Advanced Functional Materials*, vol. 19, no. 4, pp. 604–609, Feb. 2009, doi: 10.1002/adfm.200800940.

[13] Q. Zhang *et al.*, "Application of carbon counterelectrode on CdS quantum dot-sensitized solar cells (QDSSCs)," *Electrochemistry Communications*, vol. 12, no. 2, pp. 327–330, Feb. 2010, doi: 10.1016/j.elecom.2009.12.032.

[14] P. Sudhagar *et al.*, "The performance of coupled (CdS:CdSe) quantum dot-sensitized TiO2 nanofibrous solar cells," *Electrochemistry Communications*, vol. 11, no. 11, pp. 2220–2224, Nov. 2009, doi: 10.1016/j.elecom.2009.09.035.

[15] Z. Yu *et al.*, "Highly efficient quasi-solid-state quantum-dot-sensitized solar cell based on hydrogel electrolytes," *Electrochemistry Communications*, vol. 12, no. 12, pp. 1776–1779, Dec. 2010, doi: 10.1016/j.elecom.2010.10.022.

[16] S. Wang and J. Tian, "Recent advances in counter electrodes of quantum dot-sensitized solar cells," *RSC Advances*, vol. 6, no. 93, pp. 90082–90099, 2016, doi: 10.1039/c6ra19226b.

[17] C. K. Kamaja, R. R. Devarapalli, Y. Dave, J. Debgupta, and M. V. Shelke, "Synthesis of novel Cu2S nanohusks as high performance counter electrode for CdS/CdSe sensitized solar cell," *Journal of Power Sources*, vol. 315, pp. 277–283, May 2016, doi: 10.1016/j.jpowsour.2016.03.027.

[18] Z. Tachan, M. Shalom, I. Hod, S. Rühle, S. Tirosh, and A. Zaban, "PbS as a highly catalytic counter electrode for polysulfide-based quantum dot solar cells," *Journal of Physical Chemistry C*, vol. 115, no. 13, pp. 6162–6166, Apr. 2011, doi: 10.1021/jp112010m.

[19] H. J. Kim *et al.*, "Highly efficient solution processed nanorice structured NiS counter electrode for quantum dot sensitized solar cells," *Electrochimica Acta*, vol. 127, pp. 427–432, May 2014, doi: 10.1016/j.electacta.2014.02.019.

[20] H. Chen, L. Zhu, H. Liu, and W. Li, "Efficient iron sulfide counter electrode for quantum dots-sensitized solar cells," *Journal of Power Sources*, vol. 245, pp. 406–410, Jan. 2014, doi: 10.1016/j.jpowsour.2013.06.004.

[21] C. Justin Raj, K. Prabakar, A. Dennyson Savariraj, and H. J. Kim, "Surface reinforced platinum counter electrode for quantum dots sensitized solar cells," *Electrochimica Acta*, vol. 103, pp. 231–236, Jul. 2013, doi: 10.1016/j.electacta.2013.04.016.

[22] G. S. Selopal *et al.*, "Highly Stable Colloidal Giant Quantum Dots Sensitized Solar Cells," *Advanced Functional Materials*, vol. 27, no. 30, Aug. 2017, doi: 10.1002/adfm.201701468.

[23] S. Jiao *et al.*, "Band engineering in core/shell ZnTe/cdse for photovoltage and efficiency enhancement in exciplex quantum dot sensitized solar cells," *ACS Nano*, vol. 9, no. 1, pp. 908–915, Jan. 2015, doi: 10.1021/nn506638n.

[24] J. Y. Kim *et al.*, "Highly Efficient Copper-Indium-Selenide Quantum Dot Solar Cells: Suppression of Carrier Recombination by Controlled ZnS Overlayers," *ACS Nano*, vol. 9, no. 11, pp. 11286–11295, Nov. 2015, doi: 10.1021/acsnano.5b04917.

[25] M. Ye *et al.*, "Recent advances in quantum dot-sensitized solar cells: insights into photoanodes, sensitizers, electrolytes and counter electrodes," *Sustainable Energy and Fuels*, vol. 1, no. 6, pp. 1217–1231, 2017, doi: 10.1039/C7SE00137A.

[26] V. D. Dao, Y. Choi, K. Yong, L. L. Larina, and H. S. Choi, "Graphene-based nanohybrid materials as the counter electrode for highly efficient quantum-dot-sensitized solar cells," *Carbon*, vol. 84, no. 1, pp. 383–389, Apr. 2015, doi: 10.1016/j.carbon.2014.12.014.

[27] D. H. Youn *et al.*, "A highly efficient transition metal nitride-based electrocatalyst for oxygen reduction reaction: TiN on a CNT-graphene hybrid support," *Journal of Materials Chemistry A*, vol. 1, no. 27, pp. 8007–8015, 2013, doi: 10.1039/c3ta11135k.

[28] H. T. Tung, H. K. Dan, D. Thomas, H. K. Jun, and L. T. N. Tu, "The preparation of reduced graphene oxide-Cu2S by hydrothermal method for quantum dot sensitized solar cells," *Optical Materials*, vol. 139, p. 113725, May 2023, doi: 10.1016/j.optmat.2023.113725.

[29] A. K. Geim and K. S. Novoselov, "The rise of graphene," *Nature Materials*, vol. 6, no. 3, pp. 183–191, Mar. 2007, doi: 10.1038/nmat1849.

[30] J. D. Roy-Mayhew, D. J. Bozym, C. Punckt, and I. A. Aksay, "Functionalized graphene as a catalytic counter electrode in dye-sensitized solar cells," *ACS Nano*, vol. 4, no. 10, pp. 6203–6211, Oct. 2010, doi: 10.1021/nn1016428.

[31] Y. Li *et al.*, "An oxygen reduction electrocatalyst based on carbon nanotube€"graphene complexes," *Nature Nanotechnology*, vol. 7, no. 6, pp. 394–400, Jun. 2012, doi: 10.1038/nnano.2012.72.

[32] G. Biondi, D. Cazzuffi, N. Moraci, and C. Soccodato, *Geosynthetics: Leading the Way to a Resilient Planet*. London: CRC Press, 2023. doi: 10.1201/9781003386889.

[33] J. Y. Lin, C. Y. Chan, and S. W. Chou, "Electrophoretic deposition of transparent MoS2–graphene nanosheet composite films as counter electrodes in dye-sensitized solar cells," *Chemical Communications*, vol. 49, no. 14, pp. 1440–1442, 2013, doi: 10.1039/c2cc38658e.

[34] B. Yuan *et al.*, "Reduced graphene oxide (RGO)/Cu2S composite as catalytic counter electrode for quantum dot-sensitized solar cells," *Electrochimica Acta*, vol. 277, pp. 50–58, Jul. 2018, doi: 10.1016/j.electacta.2018.04.218.

[35] E. Akman, Y. Altintas, M. Gulen, M. Yilmaz, E. Mutlugun, and S. Sonmezoglu, "Improving performance and stability in quantum dot-sensitized solar cell through single layer graphene/Cu2S nanocomposite counter electrode," *Renewable Energy*, vol. 145, pp. 2192–2200, Jan. 2020, doi: 10.1016/j.renene.2019.07.150.

[36] T. Ha Thanh, D. Huynh Thanh, and V. Quang Lam, "The CdS/CdSe/ZnS photoanode cosensitized solar cells basedon Pt, CuS, Cu 2 S, and PbS counter electrodes," *Advances in OptoElectronics*, vol. 2014, pp. 1–9, Feb. 2014, doi: 10.1155/2014/397681.

[37] C. H. Champness, "Diffusion length variation in photovoltaic cells with Bridgman-grown CuInSe2 substrates," *Thin Solid Films*, vol. 515, no. 15 SPEC. ISS., pp. 6200–6203, May 2007, doi: 10.1016/j.tsf.2006.12.067.

[38] G. Jarosz, "On doubts about Mott-Schottky plot of organic planar heterojunction in photovoltaic cell," *Journal of Non-Crystalline Solids*, vol. 354, no. 35–39, pp. 4338–4340, Oct. 2008, doi: 10.1016/j.jnoncrysol.2008.06.077.

[39] O. E. Semonin *et al.*, "Peak external photocurrent quantum efficiency exceeding 100% via MEG in a quantum dot solar cell," *Science*, vol. 334, no. 6062, pp. 1530–1533, Dec. 2011, doi: 10.1126/science.1209845.

[40] G. Veerappan, W. Kwon, and S. W. Rhee, "Carbon-nanofiber counter electrodes for quasi-solid state dye-sensitized solar cells," *Journal of Power Sources*, vol. 196, no. 24, pp. 10798–10805, Dec. 2011, doi: 10.1016/j.jpowsour.2011.09.004.

[41] W. Li, S. Zhang, B. Peng, Q. Chen, and Q. Zhong, "Structurally optimized intrinsic defect carbon driven polysulfide reduction reaction for quantum dot sensitized solar cells," *Catalysis Science & Technology*, vol. 12, no. 17, pp. 5408–5417, 2022, doi: 10.1039/D2CY00890D.

[42] J. B. Zhang, F. Y. Zhao, G. S. Tang, and Y. Lin, "Influence of highly efficient PbS counter electrode on photovoltaic performance of CdSe quantum dots-sensitized solar cells," *Journal of Solid State Electrochemistry*, vol. 17, no. 11, pp. 2909–2915, Nov. 2013, doi: 10.1007/s10008-013-2210-4.

[43] W. Guo, C. Chen, M. Ye, M. Lv, and C. Lin, "Carbon fiber/Co9S8 nanotube arrays hybrid structures for flexible quantum dot-sensitized solar cells," *Nanoscale*, vol. 6, no. 7, p. 3656, 2014, doi: 10.1039/c3nr06295c.

[44] H. N. Phuong, T. Van Man, H. T. Tung, H. K. Jun, B. Van Thang, and L. Q. Vinh, "Effect of precursors on Cu2S counter electrode on the quantum dot sensitized solar cell performance," *Journal of the Korean Physical Society*, vol. 80, no. 12, pp. 1133–1142, Jun. 2022, doi: 10.1007/s40042-022-00460-8.

BIOGRAPHIES OF AUTHORS

Le Doan Duy received the master degree in physics from Can Tho University, Vietnam. He is working as a lecturer at the Faculty of Basic Sciences, Vinh Long University of Technology Education, Viet Nam. His research interests focus on developing the patterned substrate with micro- and nano-scale to apply for physical and chemical devices such as solar cells, OLED, photoanode, and theory physic. He can be contacted at email: duyld@vlute.edu.vn.

Le Thi Ngoc Tu received the Ph.D. degree in Physics from University of Science, Vietnam National University Ho Chi Minh City, Viet Nam. She is working as a lecturer at the Faculty of Natural Sciences Teacher Education, Dong Thap University, Vietnam. Her research interests focus on photoacalyst materials. She can be contacted at email: ltntu@dthu.edu.vn.

Le Tien Dat received the master degree in Electrical and Electronics Engineering Technology from HCMC University of Technology and Education, Viet Nam. He is working as a lecturer at the Faculty of Basic Sciences, University of Cuu Long, Vietnam. His research interests focus on electronics materials. He can be contacted at email: datdcnk29@gmail.com.